Application of a two-color free-electron laser to condensed-matter molecular dynamics

Dana D. Dlott

School of Chemical Sciences, University of Illinois at Urbana-Champaign, 505 South Mathews Avenue, Urbana, Illinois 61801

Michael D. Fayer

Department of Chemistry, Stanford University, Stanford, California 94305

Received October 24, 1988; accepted January 17, 1989

The possible applications of a free-electron laser (FEL), which would be modified to produce two synchronized, independently tunable picosecond pulses, are considered. At least one of the pulses would be available in the vibrational infrared region. Such an instrument would be more useful in the area of condensed-matter molecular dynamics than the conventional one-color FEL. We review briefly the dynamical processes of greatest interest in complicated, condensed-matter molecular systems. We discuss how a one-color and a two-color FEL can be used for experimental measurements of these processes and the advantages that a two-color system would have over existing technologies. We then provide a model calculation to determine the feasibility of these experimental measurements. This calculation is based on the anlysis of two-color FEL's by Schwettman and Smith [J. Opt. Soc. Am. B **6**, 973 (1989)]. Finally we examine the most promising applications of a two-color FEL and propose several specific experiments. The applications that are discussed include vibrational relaxation in molecular systems, dynamics of surfaces, photobiology and biophysics, and coherent optical measurements of intrinsically disordered materials.

1. INTRODUCTION

In a series of conversations with H. A. Schwettman and T. I. Smith, we discussed the possible uses of free-electron lasers (FEL's) in basic and applied research in solid-state physics, materials science, and biophysics. We decided that ultrafast time-resolved experiments using the pump-and-probe technique[1] would be an important application of FEL's. We could easily imagine many uses for a FEL, and these are discussed below. However we often felt constrained by a limitation of existing FEL's. Even though the FEL is tunable, its output consists of only one color at a time.

Many of the ideas discussed in this paper are the motivation for the development of a two-color FEL, i.e., a FEL that can simultaneously generate two synchronous picosecond pulses (1 psec = 10^{-12} sec) with independently tunable colors. Both pulses may be in the infrared (IR), or one may be in the IR and the other in the visible or the ultraviolet (UV) spectral range. In this issue of the journal a companion paper by Schwettman and Smith[2] discusses the technical aspects of the two-color FEL. In this paper we describe the types of applications that might be found for a FEL and the advantages of a two-color FEL system.

The original picosecond lasers[1] were based on ruby and Nd:glass. The lasers produced pulses at a single wavelength. Nonlinear crystals were used to generate the second or higher harmonics. While the development of these lasers produced a great deal of interesting science, experimenters were generally limited to the study of samples that absorbed light at the laser wavelength. The development of tunable picosecond dye lasers greatly extended picosecond spectroscopy.[3] The sample could be chosen for its intrinsic interest, and the laser could be tuned to the sample absorption. This additional flexibility made picosecond laser spectroscopy almost commonplace.

Even with tunable dye lasers, however, having only a single color proved to be another major limitation in the general application of fast spectroscopy. With a single color, a particular state can be excited, and then properties related to that state can be probed as a function of time. In many instances, as described in detail below, it is necessary to understand dynamics that involve many states of the system. It is desirable to probe a second state, which absorbs at a different wavelength. With dye lasers, this need was fulfilled by using two dye lasers pumped by a single pump laser (usually an argon-ion laser or a Nd:YAG laser). These lasers are typically limited to visible wavelengths. In addition there are often timing jitter problems, even when both dye lasers are driven by the same pump laser.[4] This jitter may reduce the time resolution well below that imposed by the duration of the laser pulses themselves.

While tunable dye lasers have gone a long way toward filling the needs of picosecond spectroscopists working with visible wavelengths, the situation in the IR is not so well in hand. Visible lasers are used predominantly to study electronic states of molecules. Vibrations of molecules have optical transition frequencies that occur in the IR, at approximately 3 to 25 μm. By using parametric processes it has been possible to use conventional laser systems to generate ultrashort pulses in the 1.6- to 3.5-μm range[5] and low-intensity pulses in the 3- to 7-μm region.[6,7]

The FEL is well known for its ability to produce tunable IR pulses that are short in duration (2 psec) and high in power (megawatts). FEL's can be tuned from the near UV

0740-3224/89/050977-18$02.00

to the far IR. A FEL can also provide high-powered pulses at a high repetition rate. These desirable characteristics will make the FEL an increasingly useful tool for basic and applied research. To date, however, FEL's produce only one wavelength at a time. It is therefore possible, for example, to excite a vibrational mode of a molecule and follow in time the flow of energy out of that mode. With a second independently tunable frequency it would be possible to tune into other states of the system and follow the flow of energy into initially unexcited states. A two-color FEL is ideal for this type of application. It could be a source of high-power, independently tunable wavelengths with little or no timing jitter between the two-color pulses. In addition the inherent pulse structure of the FEL can be usefully exploited for certain types of optical coherence experiments, which even in the visible are not possible with conventional lasers.

In the following sections, some of the considerations that define the usefulness of a two-color FEL are discussed. In Section 2 a brief introduction to molecular spectroscopy is given. This is intended for individuals who come from an accelerator physics background, an engineering background, or another discipline that does not normally deal with molecular spectroscopy, particularly in condensed phases. Those well versed in molecular spectroscopy may wish to go directly to Section 3. Section 3 describes the types of measurement methods that might commonly be employed with a two-color FEL. Section 4 gives a numerical example of one such experiment to show in detail the types of factors that must be considered and the feasibility of such experiments. Section 5 presents discussions of a number of fundamental problems that can be addressed by taking advantage of either the two colors produced by a FEL or the pulse structure of the FEL output.

None of the discussion presented below is intended to be comprehensive. Rather it should be considered a starting point in the development of experimental concepts and in stimulating the development of FEL hardware capable of producing two colors.

2. MOLECULAR SPECTROSCOPY

In this section we review some elementary concepts of molecular spectroscopy. This section is intended as an introduction to the types of dynamical processes that are important in the chemistry and physics of complicated, condensed-matter molecular systems. We cannot treat this subject in detail owing to space limitations, but many fine texts are readily available.[1,3,8–11]

A. Chemical Structure

The molecular systems studied by chemists range from the simplest diatomic molecules to biopolymers of enormous complexity. For example, a strand of human DNA is a single molecule whose extended length may be as great as 1 cm. One of the most studied systems in condensed-matter molecular spectroscopy is the naphthalene molecule, and in specific examples we will consider its properties as representative of a large variety of complex, organic, chromophoric molecules. Naphthalene is not a small molecule, like HF and N_2, but neither is it so complicated that its excited states cannot be enumerated. A sizable data base exists on the dynamical properties of naphthalene (see, e.g., Refs. 8, 10, 12) in the crystalline state and in solution. Naphthalene has also been used as a probe of the complicated dynamics that are inherent in disordered systems such as micelles, glasses, porous solids, and polymers.[13]

The structure of naphthalene, $C_{10}H_8$, is shown in Fig. 1. Its backbone consists of two fused hexagons of carbon atoms with hydrogen-atom outriggers. There are two distinct types of chemical bonds present. The C—C and C—H atoms are linked by sp^2 sigma bonds, consisting of tightly bound valence electrons that are localized in the space between the two positively charged nuclei. In addition, each carbon atom possesses one additional valence electron, which inhabits p_z orbitals perpendicular to the molecular plane. The ten p_z electrons are shared almost equally among all the carbon atoms, resulting in a delocalized π-electron system denoted by the two circles. Whenever the number of π electrons equals $4n + 2$, where n is an integer, the molecule possesses a special stability, called aromaticity.[8] Aromatic molecules are usually chromophoric, that is, they strongly absorb visible or UV light.[10] The presence of weakly bound, delocalized electrons also permits aromatic molecules to engage in a wide variety of interesting processes, such as photoconductivity and electronic energy transfer.[8]

Elementary quantum-mechanical considerations allow us to enumerate the degrees of freedom of a naphthalene molecule, which is an aggregate of 196 protons, neutrons, and electrons. However, in dealing with low-energy processes such as the absorption of light in the IR, visible, and near UV, many of these degrees of freedom can be neglected because they involve energies that are too high (e.g., nuclear) or too low (e.g., electron spin) to be of much importance. The most important degrees of freedom are those involving electronic excitations of the loosely bound π electrons and molecular vibrations. Of the latter, each of m atoms contributes three coordinates of translational motion, so that the molecule itself has $3m$–6 normal modes of vibration, three translations, and three rotations. If we take a large number N_0 of these molecules and construct a condensed-matter system, there will then exist a set of $6N_0$ bath states consisting of various combinations of low-frequency (roughly 0–200-cm^{-1}) rotations and translations. In crystals,

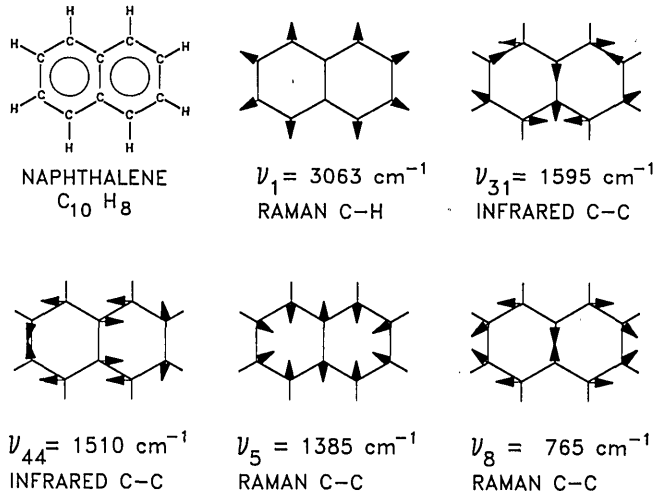

Fig. 1. Chemical structure of naphthalene and atomic displacements for a few of the 48 normal modes of vibration.

which have extended translational symmetry, these bath states are called phonons.[14] The bath plays an important role in the nonequilibrium thermodynamic processes that we will discuss: whenever a perturbation is applied to the system, for example by a FEL pulse, the system must eventually return to equilibrium. The return to equilibrium, or relaxation, occurs as the energy of the perturbation is dissipated into the bath states.

B. Electronic Absorption

Electronic absorption processes involve strong coupling of molecules with UV or visible light. Table 1 summarizes the energies of IR, visible, and UV light. In an aromatic molecule, the π electrons can be excited to higher-energy states by photon absorption. The most intense optical transitions occur between states of the same multiplicity, for example, between the ground S_0 and excited S_1 states.[8-11] The S states involve only paired electron spins, so they are singly degenerate. The $S_0 \rightarrow S_1$ transition in naphthalene occurs near 0.317 μm, in the near UV.[8] A generalized energy-level diagram for naphthalene is given in Fig. 2. The format of Fig. 2 is termed a Jablonski diagram.[9] Figure 2 shows that, in addition to the S_1 excited state, there is a manifold of higher-energy S states, denoted S_2, etc. There is also a manifold of T states, which are triply degenerate because two electrons have unpaired spins. Transitions between S and T states involve flipping the spin of one electron. Such a process is allowed only because of spin–orbit coupling, so that $S \rightarrow T$ state transitions are usually weaker than $S \rightarrow S$ or $T \rightarrow T$ transitions.

Because naphthalene absorbs in the near UV, it has the appearance of a colorless solid. In general, the more extensive the delocalized network of π electrons, the lower the energy of the S_1 state. Thus larger molecules such as chlorophyll, hemoglobin, and dyes such as Rhodamine 6G absorb strongly in the visible part of the spectrum. Visible absorption imparts color to the molecule, making chlorophyll green, hemoglobin red, and so on.

Electronic absorption spectroscopy is a routine tool in chemistry and physics.[8] Chemical compounds, particularly those with aromatic subgroups, can be identified or monitored by their characteristic absorption spectrum. Dye molecules, which interact strongly with visible light, can be identified by their spectra in very low concentration, even at the picomolar scale. However, absorption spectroscopy has an important drawback: although compounds can be identified by comparison with their known spectra, absorption spectra are typically broad and featureless. They furnish little information about the chemical structure of a molecule. Optical absorption strength is usually characterized by a cross section, σ, which has units of square centimeters. For example, one of the most strongly absorbing molecules is chlorophyll, which is used in nature as an antenna to harvest solar photons in photosynthesis. At the absorption peak of chlorophyll, $\sigma \approx 10^{-16}$ cm^2.[10] The meaning of this cross section is that the area for capture of a single photon by a single molecule is about one square angstrom (1 Å = 10^{-8} cm). This capture process is statistical in nature.

C. Vibrational Spectroscopy

Molecules are not static entities; their component atoms are constantly in motion, vibrating about their equilibrium positions. The modern view of a dynamic molecule is that the chemical bonds behave as quantum-mechanical springs that permit the bonded atoms to vibrate. The simplest picture is to consider these springs harmonic. In this case, the complex motion of the atoms can be decomposed into a small number of normal modes of vibration.[14,15] However, harmonic springs cannot be broken, and energy present in a harmonic mode will never be transfered to other modes. Thus a more accurate approximation considers the springs anharmonic.[14] It is then possible for the chemical bond to be broken by large-amplitude motions of the atoms. When energy is deposited in one mode, it is weakly coupled to all the other modes, permitting mechanical energy to flow through the molecule and ultimately to dissipate in the molecular environment.

Table 1. Energies of Optical and Chemical Processes

Optical

Photon	λ (μm)	E (cm^{-1})	E (eV)	E (kJ/mole)
UV photons	0.4–0.16	25 000–65 000	3–8	300–800
Visible photons	0.4–0.7	14 000–25 000	1.8–3	200–300
Near-IR photons	0.7–3	3000–14 000	0.4–1.8	40–200
Vibrational IR photons	3–25	400–3000	0.05–0.4	5–40
Thermal energy k_BT at 300 K	≈50	≈200	≈0.025	≈2.5

Chemical

Bond	Dissociation Energy (kJ/mole)	Vibrational Frequency (cm^{-1})
C—H		
Aromatic	400	
Stretch	–	3000–3100
Bend	–	675–870
C—C		
Aromatic	≈500	
Stretch	–	1000–1600
Bend	–	400–1000
C=O	750	1690–1760
C—N	300	1180–1360
O—H	460	3610–3640
N—H	390	3300–3500

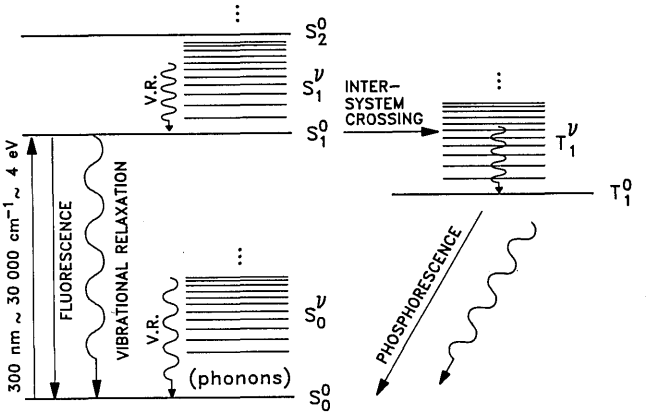

Fig. 2. Energy-level diagram showing some of the most common dynamical processes that occur in complex molecular systems in condensed phases. The straight arrows denote radiative processes; the wavy arrows denote nonradiative processes. V.R., vibrational relaxation.

Much effort has gone into the characterization and computation of normal modes,[15] as these provide a nearly complete description of the mechanical motions of molecules. Some representative normal modes of naphthalene are shown in Fig. 1, along with their fundamental frequencies.[16]

The fundamental frequency of a vibrational mode is

$$\nu_0 = (k/\mu)^{1/2}, \tag{1}$$

where k is the force constant and μ is the reduced mass of the atoms.[15] Equation (1) shows that the vibrational frequency is directly related to the mass of the atoms and to the strength of the bond. A knowledge of a molecule's vibrational frequencies is thus a powerful tool for determining the types of atoms and bonds present, i.e., the molecular structure. Table 1 summarizes the characteristic vibrational frequencies of the most common molecular bond groups found in organic matter, which consists mainly of carbon, hydrogen, nitrogen, and oxygen.[17]

There are two distinct types of vibrational spectroscopy, IR absorption and Raman scattering. Light interacts most strongly with matter when the excitation process involves a strong dipole moment. For example, vibrational excitation of a molecule such as HCl produces a large change in the dipole moment, as the H possesses a fractional positive charge and the Cl possesses an equal but opposite negative charge. Thus HCl, whose fundamental frequency is $\nu_0 = 8.8 \times 10^{13}$ Hz, strongly absorbs IR light at 2938 cm^{-1}, or 3.4 μm. The spectral region of characteristic vibrational absorptions is called the vibrational IR, located approximately between 3 and 25 μm.[17]

Symmetrical molecules such as N_2 possess no dipole moment and do not absorb IR light. However, bond displacement does affect the polarizability of the bond. Polarizability refers to the ability of a bond to form a dipole when it is subjected to an electric field. Thus, when a molecule is irradiated with a strong light field, a dipole is induced in it, and the induced dipole then can interact with the light to cause inelastic scattering. This process is called Raman scattering.[15] For example, with visible light of frequency Ω incident upon a cell of N_2, some inelastically scattered light is produced at frequency $\Omega - \nu_0$, where $\nu_0 = 2345$ cm^{-1} for N_2. The Raman effect is widely used to determine the frequencies of normal modes that are not IR active.

In large molecules, there is a mix of IR- and Raman-active vibrational modes. Group theory[15] can be used to classify the vibrations of a molecule and determine their spectroscopic activity. In low-symmetry molecules, vibrations may be both IR and Raman active, but if the molecule possess a center of symmetry, as does naphthalene, IR and Raman activity is mutually exclusive. Group theory can be used to show that naphthalene has 48 normal modes.[16] Twenty four of these modes are Raman active, twenty are IR active, and four are optically inactive.

Raman scattering also provides a unique method for direct measurement of the vibrational temperature of a particular sample.[11] Cold molecules in their ground vibrational state can only absorb energy from the optical field. Raman-scattered light from cold molecules consists of only red-shifted light at frequencies $\Omega - \nu_i$. When the emission is red shifted, the process is Stokes Raman scattering. Hot molecules may have significant populations in excited vibrational states as well as in the ground state. Hot molecules can transfer energy from their vibrations into the radiation field to produce light at frequencies $\Omega + \nu_i$. In this case the emission is blue shifted, and the process is anti-Stokes Raman scattering. If a molecule is in thermal equilibrium with a bath at temperature T, the relative populations in the ground state P_0 and first excited state P_1 are given by[11]

$$P_1/P_0 = \exp(-h\nu_0/k_BT) = (\text{anti-Stokes})/(\text{Stokes}), \tag{2}$$

where k_B is Boltzmann's constant and h is Planck's constant. Because the ratio of anti-Stokes and Stokes scattered light is proportional to P_1/P_0, an experimental determination of this ratio gives the temperature T. For example, consider N_2 at 300 K. In this case, Table 1 gives $k_BT \approx 200$ cm^{-1} and $P_1/P_0 = 8 \times 10^{-6}$. This phenomenon is often exploited for remote monitoring of the temperature in flames, in laser-heated solids, or in the upper atmosphere.

Equation (2) applies only to systems in thermal equilibrium. It is possible to create states in which certain vibrational degrees of freedom are hotter than others or hotter than the electronic or rotational degrees of freedom. The excess energy in a nonequilibrium vibrational state can be quantitatively described by Eq. (2) by substituting the vibrational temperature θ_v for the temperature T. Nonequilibrium vibrational states can be created by optical pumping or chemical reactions and are the basis for chemical lasers.

IR and Raman spectroscopies are among the most powerful available techniques for characterizing molecular structure. A great deal of effort has gone into the systematic interpretation of vibrational spectra and the correlation of the observed vibrational frequencies with the presence of specific chemical groups on the molecule. Table 1 outlines some of these chemical groups and their associated vibrational frequencies. Such tables are in everyday use in analytical chemistry laboratories. Table 1 shows that the vibrational frequency of a particular molecular group varies over a narrow range. This variation is environment specific and is caused by the details of the chemical bond and its adjacent bonds. For example, C—H of methane, CH_4, has $\nu_0 = 2914$ cm^{-1},[17] while the C—H modes of naphthalene have fundamental frequencies ranging from 3011 to 3072 cm^{-1}.[16]

IR and Raman spectroscopies have their own advantages and disadvantages. IR absorption is a fundamentally stronger interaction than Raman scattering, and the cross section for strong IR absorbers is typically 10 orders of magnitude larger than the analogous cross section for strong Raman scatterers. The small cross section is the biggest disadvantage of Raman scattering, and intense, monochromatic, visible sources (i.e., lasers) are usually necessary for observation of the Raman effect. There is an important method that boosts the intensity of Raman scattering by several orders of magnitude. When the optical frequency Ω is coincident with a molecular absorption frequency (e.g., an $S_0 \rightarrow S_1$ transition), the Raman emission is strongly enhanced. This process is called resonance Raman.[11] It is a widely employed tool for studying vibrational spectroscopy of highly colored molecules because of its sensitivity.[18] It is also highly selective because the resonance Raman effect can be used to pick out a colored molecule from a sea of colorless molecules.

The other advantages and disadvantages are rooted in the technical means used to generate and detect vibrational spectra. IR spectroscopy requires a radiation source that

must produce photons at the exact frequencies of the transitions under study. Thermal sources (hot bodies) produce wideband IR radiation whose intensity in a narrow spectral range $\Delta\nu$ is usually quite small. In addition, IR photon detectors are relatively inefficient and noisy and usually involve cryogenic cooling systems to reduce the blackbody background. There are a number of powerful IR laser sources available, but they are not easily tunable. Here the FEL stands out as a most desirable source of intense, broadly tunable, ultrafast IR pulses.

Raman scattering requires a monochromatic source, which need not be tunable. Usually the source frequency Ω is in the visible or UV. Spectral analysis of the scattered light at frequencies $\Omega - \nu_i$ is usually accomplished with a spectrometer or a spectrograph. Raman scattering typically involves the detection of high-energy visible or UV photons, and detectors in this range are usually superior to IR detectors. Conventional Raman measurements of stable species are usually made with continuous laser sources. Detection of the Raman spectrum of a short-lived, transient species requires intense ultrashort pulses that are synchronized with the pulse source that creates the transient species. Although there are many sources of ultrafast visible light pulses that are suitable for time-resolved Raman scattering,[3] the FEL again stands out because the average powers of these sources are usually measured in milliwatts, while the FEL power is of the order of watts.

D. Dynamical Processes

Consider a condensed-matter molecule initially at low temperature. It is in intimate contact with a large number of other molecules that compose the thermal bath. If we perturb the molecule, it will ultimately dissipate its energy into this bath and return to equilibrium. These perturbations and dissipations are the origin of condensed-matter dynamics. Some important dynamical processes are diagrammed in Fig. 2.

If we irradiate the molecule with light that is not sufficiently energetic to excite the electronic states, we can still produce vibrational excitation through direct absorption or Raman scattering. The vibrational states of the S_0 electronic manifold will be called S_0^{ν}. The vibrationless ground state is denoted S_0^0. In the S_0^{ν} states the molecule is vibrationally hot, and it must cool by mechanical energy transfer to other vibrations, denoted $S_0^{\nu'}$, or to the bath. The decay of energy out of S_0^{ν} is a radiationless process called vibrational relaxation (VR). Radiationless processes are denoted in Fig. 2 by wavy arrows. In complicated condensed-matter systems, VR is very fast, typically occurring in a few picoseconds (1 psec = 10^{-12} sec).[19] Usually a molecule must undergo several VR steps to return to S_0^0 from S_0^{ν}, and this multistep process is called vibrational cooling.[20]

Another possibility for producing vibrational excitation is to irradiate the molecule with light that matches the $S_0^0 \rightarrow S_1^0$ transition. In the S_1 state, π electrons have been promoted from the bonding orbitals to the high-energy antibonding orbitals. This promotion process changes the electric field potential felt by the nuclei and thus changes the force constant of each chemical bond. The vibrational excitations of the excited state, denoted S_1^{ν}, differ from the S_0^{ν} vibrations of the ground state. In the case of naphthalene, this difference is small. Some molecules undergo significant photoinduced rearrangements in their excited states. In these cases, the structure of the excited-state molecule and its normal mode is significantly different from that in the ground state. Still other molecules undergo radical, irreversible structural changes in excited states, in other words, photochemistry.

In the S_1^0 state, the molecule may relax through radiative or nonradiative processes. Radiative relaxation, denoted by the straight arrows in Fig. 2, produces fluorescent photons. Nonradiative relaxation involves coupling between S_1^0 and the large numbers of S_0^{ν} states, which are nearly isoenergetic with S_1^0, or intersystem crossing into the manifold of T states. In naphthalene, the lifetime of S_1^0 is 96 nsec.[10] On average, 23% of S_1^0 states decay by fluorescence, while the remaining 77% relax nonradiatively into T_1 or S_0^{ν} states.[10]

It is also possible for optical absorption to promote the molecule directly from S_0^0 to S_1^{ν} states. In this case, another vibrational cooling process results, but this time it occurs in the S_1 state. On the time scale of 10^{-10} sec, cooling is complete,[20] and S_1^0 is populated. S_1^0 then relaxes on the 100-nsec time scale as described above.

Intersystem crossing involves spin–flip transitions from S_1^0 to T_i^{ν}, usually an excited vibration of T_1.[9] Once T_i^{ν} is populated, vibrational cooling again occurs on the picosecond time scale to populate T_1^0. The T_1 state is only weakly coupled to S_0, so its relaxation is much slower and, depending on the details of the spin state, may take as long as 100 sec.[9] The T_1 decay may be radiative or nonradiative. If it is radiative, the accompanying emission is called phosphorescence.

An important possibility not shown in Fig. 2 is that of photochemical reactions. Table 1 shows that UV or high-end visible photons have just about the correct energy to break chemical bonds. However, the energy of a photon is rapidly redistributed through the other degrees of freedom of the molecule, and this redistribution process competes with bond breaking. Some photochemical reactions lead to direct bond cleavage, but the majority occur indirectly. In these cases, the potential barrier for the chemical reaction is smaller in the excited state than in the ground state, so the photon plays a catalytic effect by lowering the barrier.

It is of great importance to determine the rates and detailed mechanisms of these electronic and vibrational relaxation processes, as they are the fundamental processes of molecular physics and chemistry. Chemical and physical transformations are accomplished by putting excess energy into molecules, usually by heating or irradiation. The subsequent disposition of this excess energy by chemical or mechanical processes is the central topic of condensed-matter molecular dynamics.

3. ULTRAFAST MEASUREMENTS WITH THE TWO-COLOR FREE-ELECTRON LASER

There is a simple argument from classical statistical mechanics to determine the natural time scale of chemical processes. Every atom has an amount of kinetic energy equal to $E_{\text{kin}} = 3k_BT/2$. The particles in condensed-matter systems are therefore constantly moving and colliding with one another. The characteristic time, τ_c, that corresponds to this energy is $\tau_c = 2h/3k_BT$. At ambient temperature, $\tau_c = 0.17$ psec. Thus elementary chemical reaction events occur on

the time scale of approximately a tenth of a picosecond or longer. This argument does not apply to electrons, as they are inherently quantum mechanical. Some electronic processes can occur in as little as a few femtoseconds. Processes that involve picosecond or femtosecond events are called ultrafast processes. It is highly desirable to be able to measure dynamical processes on the subpicosecond and picosecond time scales.

The FEL pulses have a duration of approximately 2–5 psec, so they do not provide the ultimate time resolution sought by researchers. If pulse duration were the only important attribute of the FEL, it would not be an interesting tool. Commercial visible wavelength dye laser systems are now available at a cost of $100–$400K that provide subpicosecond optical pulses in a benchtop setup. However, the two-color FEL offers some significant advantages that benchtop lasers are not likely to match in the near future. In order to understand these advantages, it is necessary to discuss briefly how ultrafast measurements are made. We might also comment that recent advances in quantum optics have made it possible to compress optical pulses,[21] with compression factors ranging up to 10^2. Pulse compressors are lossy components that reduce the energy of a laser pulse by factors of 3–10, so the FEL is an attractive candidate for pulse compression owing to its high average power.

Figure 3 is a schematic diagram of ultrafast spectroscopic measurement techniques. The usual method of making these measurements is called pump-and-probe. A complicated laser apparatus (not shown) generates an intense ultrashort pulse, the pump, and a (usually) weaker ultrafast pulse, the probe. In many experiments, the two pulses are derived from the same laser and have identical characteristics, excepting their relative intensities. However, in general, it is advantageous to have a system such as a two-color FEL, which would produce two independently tunable pulses. Since optical pulses propagate at the speed of light,

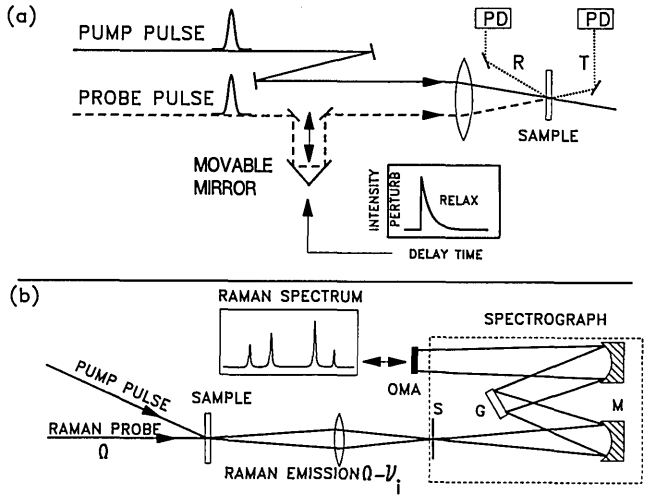

Fig. 3. Diagram of an experimental apparatus for picosecond measurements with a FEL. (a) Pump-and-probe measurements. The intense pump pulse induces a physical or chemical change in the sample, and the delayed probe pulse is used to study time-dependent changes in transmission (T) or reflectance (R). PD, photodetector. (b) In this experiment the probe method involves spontaneous Raman scattering. The Raman emission stimulated by the probe pulse is imaged through a spectrograph into an OMA. S, Slit; G, diffraction grating; M, curved mirror.

$c = 3 \times 10^{10}$ cm/sec, the physical length of the pulse, l, is directly related to its duration, $t_p = l/c$. For example, for $t_p = 3.3$ psec, $l = 1$ mm.

The role of the pump pulse is to create a sizable physical or chemical change in the sample. The pump might create an electronic or vibrational excited state; it might induce a photochemical reaction, cause a sudden jump in the sample temperature, or orient or polarize the molecules by virtue of its large electric field.[2] Once perturbed, the sample will relax. One goal of ultrafast spectroscopy is to measure this relaxation process.

Most electronic devices are not fast enough to measure ultrafast events,[1,3] so the timing in these experiments is accomplished in the following manner. The pump and probe pulses are directed into the sample by a system of mirrors, and the geometry of the system determines the path length differential for the two pulses. The probe pulse path includes at least one mirror that can be easily moved. Increasing the path-length differential increases the relative delay between pump and probe events. A 1-cm differential leads to a delay $t_d = 33$ psec. Thus the measurement of ultrafast time delays is surprisingly simple, because it involves the measurement of convenient distances in the optical apparatus.

The state being probed might be the one that was pumped, or it might be a state populated by a relaxation process. The probe pulse monitors the relaxation process in a variety of ways. The relaxing sample might exhibit a time-dependent absorbance or reflectivity. Figure 3(a) shows how absorbance or reflectivity changes can be monitored. Another observable might be Raman scattering induced by the probe pulse at frequencies $\Omega \pm \nu_i$. Figure 3(b) shows how the Raman spectrum of a perturbed sample can be acquired by using a spectrograph to analyze the spectral content of the emission and an optical multichannel analyzer (OMA) to detect the Raman emission. It is also possible to detect time-dependent fluorescence from a sample by using either fast photoelectronic systems (streak cameras[1] or time-correlated photon counters[3]) or optical sampling in a nonlinear crystal.[22]

In the apparatus of Fig. 3(a) the signal waveform corresponding to the sample relaxation process is reconstructed by the technique of sampling. Sampling is possible only when the laser produces a repetitive stream of nearly identical pulses. First the movable mirror is set so that the two arms of the optical system are equal, corresponding to $t_d = 0$. The laser is then pulsed, possibly several times, and the probe pulse is detected. Then the mirror is moved to a new location, say 1 mm, and the probe is again detected. This yields the experimental value for 3.3 psec of delay. The process is repeated at many delay values, including values of $t_d < 0$ that establish the baseline. In this manner, the signal waveform is reconstructed. With a FEL it would be desirable to accumulate data from all the micropulses occurring during a single macropulse. In the interval between macropulses the mirror can be moved to a new location by using a stepper motor.

In the apparatus of Fig. 3(b) the OMA simultaneously detects Raman-shifted emission at many different wavelengths. For a given value of t_d the OMA obtains the entire Raman spectrum of transient species created by the pump pulses. Typically the emission from several macropulses would be integrated in the OMA to obtain a spectrum.

The above discussion allows us to discern some of the most desirable qualities of a laser source for ultrafast measurements. First, production of two independently tunable, simultaneous laser pulses is highly desirable. The use of two different pulses permits the experimenter to choose wavelengths that individually optimize the pump and probe processes. Second, for many experiments, the pulses need to be extremely powerful. The second consideration follows from the ultrashort duration of the pulses and the necessity to produce a detectable perturbation in the sample with the pump pulse. The power requirement has led to the design of ultrafast lasers whose peak pulse powers are in the megawatt or gigawatt regime. Finally, the pulses should be repetitive and reproducible, with a repetition frequency adequate for reconstructing and averaging the signal waveform in a reasonable amount of time.

There are several elements of the two-color FEL that make it highly desirable for ultrafast dynamic studies: first, the availability of synchronous pulses at two frequencies, at least one of which can be in the problematic vibrational IR; second, the ability for either or both frequencies to be tuned over a wide range exceeding that of conventional lasers; and finally, the nature of the FEL output, a consequence of the linear accelerator used to pump the FEL. (We are referring here to the FEL at Stanford University.) The FEL pulses have megawatt peak powers, sufficiently powerful to induce sizable chemical or vibrational changes in a sample. The long accelerator produces an interpulse spacing of approximately 85 nsec, which is nearly ideal.

The pulse-repetition frequency is an important parameter in ultrafast spectroscopy. The FEL repetition frequency is far greater than that of other megawatt laser sources, giving high average power. However, a too-large repetition frequency is undesirable. In most measurements, the optimum frequency is the maximum that allows the sample to return to the ground state during the interpulse interval. Nearly all systems require a minimum of a few tens of nanoseconds for this return process, so interpulse spacings much less than this value are often undesirable. For some samples, it will be necessary to increase the interpulse spacing still further. This reduction can be accomplished with an optical modulator with a rise time of a few tens of nanoseconds. Modulators with rise times in this range are widely available from commercial sources, whereas systems with rise times much less than 10 nsec involve much more complicated switching techniques.

The IR part of the FEL can operate in most of the vibrational IR, including the critical 2.8–15-μm region. It should be highly efficient in the near IR, where semiconductor intraband transitions lie. The visible part of the FEL can operate throughout the entire visible spectrum. By using conventional frequency multiplier crystals the range can be extended into the UV. Only a few existing lasers can produce sizable tunable IR pulses. The most common technology involves optical parametric generation in $LiNbO_3$ crystals,[5] but these crystals have an effective range of 1.6 to 3.5 μm, making most of the vibrational IR inaccessible. Although other IR materials are under development, high-power tunable ultrafast pulse systems in the vibrational IR do not yet exist. Furthermore, existing IR systems produce average powers of a few milliwatts, compared with watts for the FEL.

Tuning the visible part of the FEL involves electronic adjustment of the electron-beam energy. It will also be necessary to change the two mirrors of the laser resonator for large-wavelength excursions. We anticipate that it will be easier to tune the FEL over a wide range than to tune an amplified, ultrafast dye laser. In a dye-laser system of this sort,[3] wide-wavelength excursions may involve replacing the dye-laser mirrors (there are usually three to seven), changing the dye and amplifier gain and saturable absorber dyes, and possibly several layers of mechanical readjustments. A conventional dye-laser system produces nanojoule pulses at high (megahertz) repetition rates[3] or microjoule pulses at kilohertz rates,[23] in either case giving average powers in the milliwatt range. Benchtop dual dye-laser systems have difficulty obtaining high time resolution when it is necessary to produce two high-power, independently tunable pulses. Even when two identical dye lasers are pumped by the same master oscillator, timing jitter exists between pulses from the two lasers.[3,4] The FEL may experience less jitter because of close correspondence between the electron bunches and the optical pulses.

One of the most promising applications for the FEL is in the study of VR. Most ultrafast experiments are performed on electronic transitions that have large absorption cross sections. However, electronic spectra, which are often broad and structureless, are not a good tool to characterize molecular structure. Ultrafast vibrational data are usually more desirable because of the fingerprint nature of vibrational spectroscopy. However, vibrational spectroscopy must employ either tunable IR pulses, which conventional lasers cannot readily produce, or Raman scattering, which has a small cross section and requires high average power. These limitations are directly overcome by the FEL.

A wide variety of experiments will be feasible when the two-color FEL is used. For convenience, we have divided these experiments into six general classes.

1. *High-power IR.* It is often desirable to irradiate systems with high-power IR light to cause nonequilibrium heating effects, such as resonant desorption from surfaces. The only high-power ($\geq$10 W) systems in the IR are a few chemical lasers restricted to relatively narrow frequency ranges. By contrast, the FEL is a broadly tunable source spanning much of the near and vibrational IR.

2. *Infrared pump and probe.* In this case a vibration of the electronic ground state, S_0'', is excited, and the rate of VR is probed with a delayed pulse of the same frequency. With the powers provided by the FEL and tight focusing, high levels of excitation can be created in all vibrations with reasonable IR cross sections.

3. *IR pump and visible probe.* In this case IR light is used to excite a vibration or to jump the temperature of the system. Visible or UV probes monitor the subsequent dynamics through absorption, fluorescence excitation, or Raman scattering.[24] Raman detection is currently difficult but should become straightforward given the high average powers of the FEL.

4. *Visible pump and IR probe.* The IR spectroscopy of short-lived transient species is virtually a nonexistent field. A visible pulse will excite molecules or initiate a chemical reaction, and IR spectra of the resultant transients can be observed by direct IR absorption changes of the probe pulses on a picosecond time scale.

5. *Visible pump and visible probe.* Many researchers

are now using this technique with benchtop laser systems, so it is only reasonable to comtemplate experiments for which the FEL provides unique advantages over conventional lasers. Here the area of excited-state Raman scattering stands out. In this experiment, a visible pulse is used to excite a molecule or initiate a chemical reaction, and the transient species thus produced are detected by Raman scattering. For high sensitivity and high time resolution to be achieved, the pump and probe pulses must both be quite intense and synchronized. Dual dye-laser systems produce average powers in the milliwatt range, and jitter between the dye lasers usually limits time resolution to ~25 psec.[3] Only in a few cases has the time resolution of time-resolved, spontaneous Raman scattering exceeded this value.[25] The FEL will permit Raman detection of low-concentration species with a time resolution of perhaps 2 psec.

6. *Nonlinear-optical interactions.* The high peak power of the FEL allows nonlinear interactions to be exploited efficiently. In these experiments, several input pulses interact in the material medium to generate output pulses at new frequencies or in different directions. Important examples are transient gratings[26] and other four-wave mixing experiments and photon echoes.[27] All these experiments can be extended to the study of condensed phases in the IR regime with the FEL, and new experiments involving various combinations of IR and visible pulses will also be possible.

4. ULTRAFAST EXPERIMENTS: A NUMERICAL EXAMPLE

Here we wish to provide a model calculation of the signal levels that can be obtained in two-color FEL experiments. For the example, we will choose the case of IR excitation and Raman probing. Of the experiments listed above, this is probably the most difficult and demanding, and a demonstration that the two-color FEL can accomplish this experiment should be taken as confirmation that the other types of experiment are at least equally feasible.

The proposed experiment follows the general design of Fig. 3. Using a tunable, picosecond IR pump pulse, a specific mode $S_0{}^{\nu}$ (see Fig. 2) is excited. Vibrational relaxation will cause the energy in mode ν to dissipate into the $S_0{}^{\nu'}$ modes of the molecule. Ultimately the ν' excitations will dissipate into the bath. The excitations of ν' will build up as ν relaxes and then decay with the VR lifetimes of ν'. Experiments that can probe the flow of mechanical energy through the ν' states would provide information about molecular dynamics hitherto impossible to obtain.[20]

The nonequilibrium populations arising in the ν' states can be probed by IR or Raman methods.[24] In the IR case, the apparatus of Fig. 3(a) is used. The probe pulse is tuned to the frequency of ν'. In an unperturbed sample the probe will be absorbed and attenuated by a known amount given by Eq. (3) below. In a perturbed sample ν' will become vibrationally hot, and the probe pulse attenuation will decrease. At large pumping levels, the probe pulse may be amplified by stimulated emission. The amount and time dependence of ν' excitation can then be determined by the time-dependent attenuation of the probe pulse.

When ν' is a Raman-active vibration the apparatus of Fig. 3(b) is used. In the unperturbed sample ν' is not excited, and mostly Stokes emission is observed. However, in a perturbed sample, anti-Stokes emission, the hallmark of excess vibrational population, will be enhanced.

It is the latter case, IR pumping and Raman probing, that we shall consider. We choose this example for several reasons. First, it is a worst-case scenario, because Raman probing is much less sensitive than IR probing. Second, Raman probing is inherently advantageous. When ν relaxes into many ν' states, IR probing techniques demand that measurements be made with the FEL tuned to each of the ν' IR frequencies. Raman probing with an OMA detector provides simultaneous information about all the ν' modes. Finally, it is straightforward to calibrate the experimental apparatus for absolute determination of the vibrational temperature of each ν' mode, $\theta_{\nu'}$. With IR probing it is certainly possible to relate the probe pulse attenuation to the vibrational temperature, but such a relation involves many parameters, including the number density, cross section, refractive index, and geometric factors. With Raman probing the spectrograph can be set to monitor the Stokes and anti-Stokes frequencies, giving a direct, absolute measurement of the vibrational temperature of each ν' mode.[28]

The IR pump-Raman probe technique has been demonstrated by Gottfried and Kaiser in Munich.[28] They studied solutions of naphthalene and anthracene in a solvent, CH_2Cl_2, whose vibrational modes interfered little with observation of the naphthalene vibrations. They used a unique laser apparatus consisting of a mode-locked Nd:glass laser that produced a 50-mJ, 6-psec pulse at 1.054 μm. The extremely large peak power of this pulse, ≈8 GW, permits the generation of synchronous pulses at other frequencies through various nonlinear processes. A disadvantage of this system is that large glass lasers such as those described in Ref. 24 cannot usually be operated at rates exceeding one pulse per minute. Experiments involve long, tedious periods of signal averaging, especially in light of the fact that each laser pulse provided roughly one photon of anti-Stokes signal. This type of experiment is so difficult with conventional laser systems that no real attempts have been made systematically to explore the effects of exciting several different ν states in the same molecule or to study a series of related compounds to learn the relationship between chemical structure and vibrational energy flow.

In the naphthalene experiments, C—H stretching vibrations were excited with a tunable IR pulse generated by parametric three-photon processes in crystals of $LiNbO_3$. Raman-active vibrations were probed, using the harmonic of the 1.054-μm laser pulse at 0.537 nm, in the green portion of the visible spectrum. The IR pulses generated in $LiNbO_3$ had an excessively large frequency bandwidth of ≈20 cm^{-1}, compared with the uncertainty limit of ~1 cm^{-1} for a 6-psec pulse.[1] For this reason two different C—H modes, at 3048 and 3064 cm^{-1}, were simultaneously excited, somewhat complicating the analysis of the experiment. The Raman probe process was used to study the behavior of three other modes, ν_1, a C—H stretching mode at 3058 cm^{-1}, ν_5 at 1380 cm^{-1}, and ν_8 at 765 cm^{-1}. These three modes are diagrammed in Fig. 1. The last two are symmetric stretching modes of the C—C skeleton. Thus the dynamic processes under investigation involve energy redistribution among the C—H modes and energy transfer from C—H modes to lower-energy C—C modes.

The results showed that within 0.5 psec the ν_1 mode be-

came excited by intramolecular vibrational energy transfer from the IR-active modes. By using the absolute calibration provided by the Raman process, it was found that 10% of the initially absorbed energy was transferred to ν_1. Because naphthalene has eight C—H stretching modes, this information was used to conclude that the initial energy was redistributed in a roughly evenhanded manner through all the C—H modes. The energy decayed out of ν_1 within 2 ± 0.5 psec. The ν_5 and ν_8 data showed that vibrational energy built up and then decayed to still lower-energy modes. The buildup for the higher-energy ν_5 occurred within 5 psec, and the decay took 9 psec; the total excitation was very small, only 1%. The buildup of ν_8 took 10 psec, the decay took 7 psec, and the amount of excitation was 10%.[28]

Such detailed information about mechanical energy flow through molecules had never before been obtained. Understanding this energy flow has been a long-standing goal of chemistry. A good data base is the prerequisite for the development of a general approach to energy flow in condensed phases such as the theory of Hill and Dlott.[20] This approach used a master equation to describe vibrational cooling in a molecular crystal such as naphthalene.

For our feasibility calculation, we will use two-color FEL parameters from Smith and Schwettman[2] corresponding to a low-energy electron beam of 21 MeV and a high-energy beam tunable to a maximum of 59 MeV. This combination, together with third-harmonic generation processes, will produce an IR pulse tunable between 5 and 15 μm, corresponding to the range of 650–2000 cm^{-1}, and an associated near-IR or visible pulse in the 2.0- to 0.67-μm range. The latter pulse can be further shifted into the UV by using standard frequency-doubler crystals. The micropulse energies are estimated at 5 μJ with durations $t_p \approx$ 2–5 psec, giving peak powers in the megawatt regime. Preliminary experiments performed at Stanford University suggest that the micropulses are approximately transform limited. Assuming a Gaussian pulse envelope, the 2–5-psec pulse duration transforms into a frequency bandwidth of $\Delta\nu \approx 3$–$8\ cm^{-1}$. We will assume a macropulse repetition frequency of 10 Hz with an overall duty cycle of 10%. In this case, the two-color FEL output will consist of 10 macropulses per second, each macropulse lasting 10 msec. The macropulse will contain $\approx 1 \times 10^5$ micropulses spaced by ~85 nsec, and at 5 μJ per pulse each macropulse has an energy of 0.5 J, with the time-averaged power of the system being 5 W in each beam. We will also keep in mind that this estimate represents an upper limit to the power delivered to the sample, as the FEL beam must travel a complicated path containing many optical components as it is transported from the source to the user laboratories. Although the optical loss of each component is minimal (perhaps a few percent), the combined effect of a large number of components is not.

With an IR pulse tunable between 600 and 2000 cm^{-1}, it would be possible to excite individually more than 10 different, strongly IR-active skeletal modes of naphthalene. The FEL must be carefully tuned into each desired IR transition with an absolute accuracy equal to the laser bandwidth of a few inverse centimeters. For this reason, a conventional IR spectrometer would be a useful accessory in a well-equipped FEL laboratory. The Raman probe need not be carefully tuned. In fact, given that optical array detectors are most efficient in the 0.4–0.9-μm range, any probe wavelength in this range is acceptable. The mechanics of the FEL are such that the choice of a particular IR wavelength will somewhat limit the choice of visible wavelengths, so we will wish to operate where the visible power is maximum. Naphthalene has 24 Raman-active modes that can be probed, although only 10 or so have really large cross sections.

The naphthalene sample may be used in several forms. Theoretically speaking, the optimal system is a perfect crystal of pure naphthalene cooled to below 10 K. It would be most desirable to study the cold crystal and then investigate the effects of raising the temperature. If an experiment is to be performed at room temperature, where $k_BT \approx 200\ cm^{-1}$, thermal population of the lowest-frequency vibrations would tend to obscure the nonequilibrium populations created by the pump pulse. Low-temperature experiments would require an optical cryostat chilled with liquid helium, with windows that pass both visible light and IR light out to 600 cm^{-1}. A good choice for windows would be ZnSe, which is hard and durable, which survives many thermal cycles without fracturing, and which is transparent in the range 0.6 to 22 μm. For some experiments, it might be desirable to dilute the naphthalene, either to avoid samples with overly large optical densities or to investigate the influence of external solvent matrices on the VR process.[12] In the solid state, pure naphthalene can be diluted by suspending microcrystals in a pressed pellet of KBr or by forming commensurate cocrystals such as 1% naphthalene in a single crystal of tetramethylbenzene (durene). Solutions of naphthalene can be studied at ambient temperature by using solvents such as CH_2Cl_2, which have wide regions of infrared transparency. The solutions could be contained in NaCl or ZnSe cells.

The first criterion for our calculation is that the IR pulse must make a sizable perturbation in the vibrational population of the sample. In other words, we require that a significant portion of the ground vibrational states be excited to the first excited state. In order to perform this calculation, we need to review briefly the equations that govern optical absorbance. We first assume that the vibrational transition may be treated as a two-level system, the ground state and the first excited vibrational level. This approximation is not adequate for harmonic oscillators, as their energy-level structure is a ladder of equally spaced levels, but is adequate for anharmonic oscillators[14] in which the energy splitting between the ground and first excited states is larger than that between the first and second excited states.

If the irradiating light is weak, its absorbance is governed by the Beer–Lambert law:

$$I(\lambda)/I_0(\lambda) = \exp[-n\sigma(\lambda)l] = 10^{-c\epsilon(\lambda)l}. \quad (3)$$

In Eq. (3), $I_0(\lambda)$ is the intensity of irradiating light at wavelength λ, $I(\lambda)$ the intensity of that light that is transmitted through the sample, n is the number of absorbing molecules (cm^{-3}), $\sigma(\lambda)$ is the absorption cross section (cm^2), and l is the optical path length (cm). An alternative way of expressing these quantities uses c, the concentration in moles/liter, l in centimeters, and $\epsilon(\lambda)$, the decadic molar extinction coefficient in liters/mole/centimeter. The appropriate, and quite useful, conversion factor is $\sigma = 3.81 \times 10^{-21}\ \epsilon$.[10] Another useful quantity is optical density (OD) [$OD = -\log_{10}(I/I_0)$]. When the OD is unity, 90% of the irradiating light is absorbed.

When the irradiating light is strong, it is possible to saturate the transition. When saturation occurs, the rate of excited to ground transitions becomes comparable with the rate of ground to excited transitions. If we consider IR pulses whose duration is short relative to the rate of VR, the fluence (J/cm^2) necessary to excite $1/e$ of the molecules is called the saturation fluence, W_{sat}, given by

$$W_{sat} = h\nu/\sigma. \tag{4}$$

Equation (4) shows that $1/e$ of the molecules are excited when the fluence is equal to the energy of one photon per cross section.

In the design of this experiment, we will begin by assuming that the sample OD, at the frequency of the pump pulse, is of the order of unity, while the pump pulse fluence is of the order of W_{sat}. The assumption is justified below. If the OD is significantly greater than unity, all the pump is absorbed on the front face of the sample; if less than unity, most of the pump energy passes harmlessly through the sample.

The critical parameters in this calculation are the cross sections for IR absorption and Raman scattering. The cross sections for the various molecular vibrations can vary over a wide range, and typically some transitions are strong while others are considerably weaker. Furthermore, these cross sections usually decrease with increasing temperature. Temperature broadens the absorption profile, reducing the cross section at the absorption peak. In low-temperature naphthalene, the most intense IR transition is the out-of-plane C—H bending mode near 800 cm^{-1} and its cross section $\sigma \approx 10^{-16}$ cm^2.[29] There are other lines with $\sigma \approx 10^{-17}$ cm^2, including ν_{31} and ν_{44} shown in Fig. 1. Other IR transitions have even lower values of σ, and one can expect σ to decrease by perhaps an order of magnitude as T is increased to 300 K.

Let us consider the specific case of excitation of ν_{31} or ν_{44} at low temperature with $\sigma = 10^{-17}$ cm^2. Given an IR pulse of 5-μJ energy near 1600 cm^{-1}, $W_{sat} = 3 \times 10^{-3}$ J/cm^2. This value of W_{sat} implies a laser beam area of 1.7×10^{-3} cm^2, corresponding to a Gaussian beam diameter of $D = 450$ μm, which is easily accomplished. In passing, we might note that the FEL has a high degree of spatial coherence and in principle can be focused to the diffraction limit, which is of the order of one wavelength, or a diameter of roughly 20 μm at 1600 cm^{-1}. In this case, the irradiated area is $\sim 3 \times 10^{-6}$ cm^2, implying that transitions as weak as $\sigma = 3 \times 10^{-20}$ can be saturated with tight focusing. However, tight focusing will present some practical difficulties involving misalignment or optical damage.

For $\sigma = 10^{-17}$ cm^2, achieving a nominal OD of unity is simple. For naphthalene, $n \approx 5 \times 10^{21}$ cm^{-3}, so a pure crystal of naphthalene will achieve the requisite value of OD when $l = 0.5$ μm. Alternatively, a convenient $l = 1$-mm path length can be achieved by diluting the naphthalene by a factor of $\sim 10^3$. Pure 1-mm samples will be satisfactory for small values of $\sigma \approx 10^{-19}$.

Assuming that we have pumped the vibrational transition to near saturation levels, we must now consider the anti-Stokes Raman probing process. Unlike in absorption processes, Raman scattered light is incoherently emitted over a wide range of solid angles. The scattering process is characterized by the differential Raman cross section, $d\sigma_R/d\theta$, where θ is the solid angle in steradians. Given a pulse with a fluence W (photons/cm^2) irradiating a volume containing N Raman-scattering centers in the ground state, the number of Stokes-scattered photons into a solid angle θ, $N_{St}(\theta)$, is given by[11]

$$N_{St}(\theta) = WN\sigma_R. \tag{5}$$

The most intense Raman transitions in naphthalene have $d\sigma/d\theta \approx 10^{-29}$ cm^2 sr.[29] One example of a strongly Raman-active mode is ν_5 (see Fig. 1). Naphthalene has approximately five modes with comparable cross sections and more than ten other modes whose cross sections are down by about an order of magnitude.

Assuming that we have optimized our pumping process, the sample has absorbed roughly 5 μJ of energy in a cylindrical volume 400 μm in diameter and perhaps 1 mm deep, corresponding to a sample volume of $V = 10^{-4}$ cm^3. At 1600 cm^{-1}, a 5-μJ pulse contains 1.6×10^{14} photons, so the concentration of vibrationally excited molecules is $N \approx 10^{18}/cm^3$. We now assume a Raman probe pulse of 5 μJ at 0.8 μm with a flux $J_0 = 2 \times 10^{16}$ photons/cm^2. Assuming for the moment that every vibrational excitation that was created by the IR pump has been transfered to ν_5, the number of anti-Stokes scattered photons from a single probe pulse is $N_{aS}(\theta) = 20$. Now we assume a reasonable aperture for the spectrograph [see Fig. 3(b)] of $f/4$, corresponding to a solid angle of ~ 0.05 sr. Thus each probe pulse scatters one photon into the detector at the frequency $\Omega - \nu_5$. We should then expect a factor-of-10 reduction to account for the quantum yield of the detector and losses in the spectrograph and collection optics.

We conclude that the combination of a strong IR transition with $\sigma = 10^{-17}$ cm^2 together with a strong Raman transition with $\sigma_R = 10^{-29}$ cm^2 sr will produce roughly 10^{-1} counts, where a count is the electronic equivalent of a detected photon. Recalling that the repetition rate of the micropulses is $>10^6$/sec, we would expect of the order of 10^5 counts/sec at a detector whose intrinsic noise level is only a few counts per second. This is an acceptable signal. Many Raman experiments are now performed with signal levels of only a few counts/second.

The value of 10^5 counts/sec is dependent on three critical factors, the IR cross section of the vibration that is pumped, the Raman cross section of the vibration that is detected, and the efficiency of energy transfer from the pumped mode to the probed mode. With the results of Gottfried and Kaiser as a guide, the last-named quantity ranges from 0.01 to 0.1,[28] reducing the signal level proportionately. The signal that remains is still large and will remain so even if the IR or Raman cross section is lowered by 1 or 2 orders of magnitude.

We can thus conclude that it is possible to perform the IR pump-Raman probe experiment on condensed-matter systems by using the two-color FEL and that the pulse properties of the FEL are so favorable that the experiment can be performed on samples with only moderately large IR or Raman cross sections or molecules in solution whose number density is reduced by a dilution factor of a few orders of magnitude.

5. PROPOSED EXPERIMENTS WITH A TWO-COLOR FREE-ELECTRON LASER

In this section we will discuss some of the most promising applications of the two-color FEL in the study of dynamical processes in complex molecular systems. We make no attempt to be complete; instead we have selected some areas that are being actively pursued in our research groups or areas in which in our opinion the two-color FEL has the greatest potential for important breakthroughs.

A. Vibrational Relaxation in Molecular Systems

One of the most important goals of chemistry is to understand how energy is disposed among the various degrees of freedom as a result of perturbations caused by optical or thermal excitations or by chemical reactions. We can distinguish three broad classes of experiments: studies of VR in simple, ordered systems such as pure crystals; studies of VR in complex systems, such as polymers and glasses; and studies of VR processes occurring during chemical reactions.

Molecular crystals are the natural starting point for fundamental studies of VR in condensed phases. Our knowledge of VR processes in molecular crystals derives mainly from spectral line-shape or coherence decay studies.[19,20] The width of a spectral transition is proportional to the rate of loss of the phase memory of the two states. This vibrational dephasing process involves two components: VR, consisting of processes that result in energy flow out of the excited state, and pure dephasing, processes that result only in loss of phase memory.[19,20] To date, there are practically no direct measurements of VR in molecular crystals; rather, VR rates have been inferred from dephasing measurements. It has not been possible experimentally to decompose the coherence decay into its VR and pure dephasing components or to measure independently the temperature dependence of each process.

By using the IR pulses from the FEL, it will be possible to measure directly the vibrational lifetime of individual states. These measurements can be performed by single-wavelength pump-and-probe or by using more sensitive, albeit more sophisticated, methods, such as transient gratings. In combination with conventional measurements of the optical line shape, the relative contributions from VR and pure dephasing are determined. The pure dephasing can be further separated into homogeneous and inhomogeneous components, and experimental resolution of these two components can be performed by using IR photon echoes (see Subsection 5.D).

The next logical step would be to study the VR process in several modes of the same molecule. The goal here would be to develop a qualitative understanding of the relationship between the amount of excess vibrational energy and the VR rate, and the dependence of the VR rate on the structure of the molecule and its crystalline environment.[20] For chemists, it is straightforward to prepare a series of chemical compounds that differ in structural details or in the way in which the molecules pack to form a crystal. For example, one might study the effect on VR of substituting deuterium for one or more of the hydrogen atoms of naphthalene[29] or investigate the VR of polymers by studying a series of crystals composed of monomer, dimer, trimer, etc.[30]

The final step would be to apply techniques such as IR pump-Raman probe[24] to determine the disposition of vibrational energy after it leaves the pumped mode and relate the dynamics of the vibrational cooling process to such structural parameters.

VR can play an important role in determining the rates of chemical reactions. This role can be quite direct, for example, in I_2 recombination.[31] In this reaction, a fluid solution of I_2 is excited with visible light, which breaks the I–I bond to form two iodine atoms. When two atoms meet, they attempt to re-form the chemical bond. However, two atoms cannot form a chemical bond without the intervention of a third atom to carry away some excess energy. Thus iodine-atom recombination in a solvent produces I_2 in a highly excited vibrational state. The loss of this vibrational energy may be the pivotal step in bond formation. It is greatly desirable to study photochemical reactions with the FEL. Nonequilibrium vibrational populations produced by a reaction that is initiated with a visible or UV pulse can be studied with IR or Raman probing. The most interesting systems for preliminary work are the simplest, for example, I_2 in the monatomic solvent liquid xenon. Such experiments will definitively distinguish the major theoretical models of collisional energy transfer in condensed phases, where many-body or correlation effects may dominate.

VR may also play a more indirect role in determining the outcomes of chemical reactions by influencing the motion of the reactant over the potential barrier. In the total absence of VR, no reaction occurs. Instead, an excited reactant will cross the potential barrier in a ballistic manner and will not fall into the potential well that defines the product state. If we can increase the rate of VR, the chemical reaction rate will increase. It will become possible to dissipate the energy of activation and populate product states. However, the increase in chemical reaction rate with increasing VR is not without limit. Ultimately the VR rate becomes large compared with the time required to cross the barrier. In this case the molecule is rapidly scattered, so its transit over the barrier becomes diffusive, again reducing the reaction rate.[32] Although there is a vast amount of information on the rates of chemical reactions, this phenomenon has never been systematically investigated because there is little accompanying information on the analogous VR rates. It is no exaggeration to say that the availability of the two-color FEL would provide one of the most important new tools that could be brought to this problem.

B. Surface Science

Surface science is one of the most rapidly advancing scientific areas. Surfaces play an active role in interfacial phenomena, heterogeneous catalysis, corrosion, lubrication, adhesion, and materials processing. A fundamental problem in surface science is that in most macroscopic materials the ratio of bulk to surface material is large. There is not much surface to study. Again, the FEL stands out because its high average power enhances the sensitivity of spectroscopic methods.

One technique that has played an important role in the development of modern surface techniques has been the deposition and subsequent desorption of molecules on clean surfaces of single crystals. The most common technique is thermal desorption. However, thermal desorption is not

highly specific because all chemical adsorbates are heated equally. The availability of intense, tunable IR radiation from the FEL suggests the possibility of IR resonant desorption. If two different chemical species coexist on the same surface, a laser tuned into a specific vibrational mode of one species might selectively desorb that species. In other words, the FEL might be used to perform microscopic surgery on surfaces by selectively removing desired molecules. The realization of this possibility depends on the vibrational dynamics of adsorbed molecules. If vibrational energy transfer from adsorbate to surface is fast, all molecules are heated equally even if only some of them are pumped by the laser. If the energy transfer is slower, molecular specificity will be achieved.[33,34]

It would also be interesting to compare the VR rates of molecules adsorbed on surfaces with VR measurements in bulk media. If the molecule is intimately bonded to the surface of a solid, its VR might be extremely fast because of efficient mechanical energy transfer to the bulk. On the other hand, if the molecule dangles from the surface, VR might be extremely slow. We can surmise that different vibrations of the same adsorbate molecule might have vastly different VR rates, and these rates might have an important influence on catalytic surface properties.

Recently Heilweil *et al.* made the first direct measurement of the VR of molecules on surfaces.[35] They used a Nd:YAG-pumped optical parametric oscillator that could be tuned in the vicinity of 3 μm and that produced pulses of $\approx$20-psec duration. This IR pulse served as both the pump and the probe, and by detecting the delay-dependent attenuation of the probe pulse in the geometry of Fig. 3(a) they determined the lifetime of O—H groups on the surface of silica, SiO_2.

SiO_2 is a giant molecule consisting of tetrahedral arrays of SiO groups. The molecule can be terminated at its surface in several different ways, as shown in Fig. 4. The surface VR experiments focused on the isolated O—H groups. The fundamental frequency of O—H is in the vicinity of 3600 cm^{-1} both in silica and in many alcohols. The VR lifetime of O—H in simple alcohols, for example, methanol, is of the order of 20 psec, while the lifetime of O—H on the surface of silica is longer by an order of magnitude, roughly 200 psec.

Heilweil *et al.* have rationalized the long lifetimes of the surface groups, using an energy-gap argument. The 3600 cm^{-1} of excess energy must ultimately dissipate into the bulk silica. However, the vibrational frequencies in the bulk are much lower than 3600 cm^{-1}, ranging from 440 to 1060 cm^{-1}. Thus vibrational energy flow out of O—H must involve simultaneous excitation of at least four bulk modes. The anharmonic matrix elements that couple different vibrational modes decrease rapidly with quantum-number mismatches, i.e., one mode goes to four modes, and thus the large energy gap between the O—H mode and the nearest energetic match at 1060 cm^{-1} is responsible for the long lifetimes on the surface.

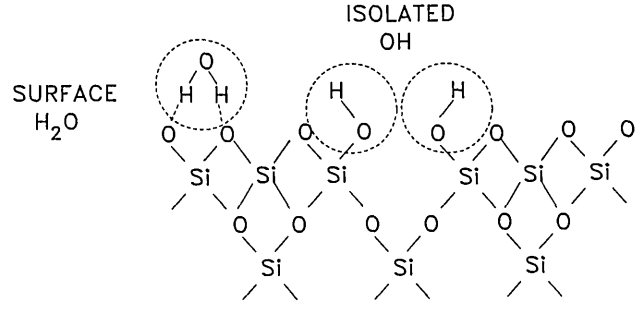

Fig. 4. Chemical structure of some of the dangling groups on the surface of SiO_2. Vibrational relaxation measurements of surface groups by Heilweil *et al.*[35] showed surprisingly long relaxation lifetimes.

The slow rate of vibrational energy transfer also has some interesting implications for surface chemistry. It has generally been assumed that catalytic reactions at surfaces occur in thermal equilibrium, and in this case kinetic rate constants are expected to obey the Arrhenius law, rate α $\exp(-E_a/k_BT)$, where E_a is the activation energy necessary to surmount the reaction barrier. It was suggested by Heilweil *et al.* that when a molecule is adsorbed onto a surface its vibrational groups do not instantaneously lose their energy, so that the vibrational temperature θ_v might be much higher than the bulk temperature T, giving a boost to the chemical reaction.

These experiments suggest many uses for the FEL in surface science. First it would be interesting to probe the energy flow into the low-frequency modes of the bulk medium with an IR pump-Raman probe or to probe the VR lifetimes of the lower-frequency bulk modes, an experiment that requires IR pulses at lower frequencies than those available with conventional lasers.

Finally, VR processes accompanying the binding or desorption of surface adsorbates could also be studied with the FEL. In a preliminary experiment using the Mark III IR FEL at Stanford University, Tro *et al.*[33] studied the IR desorption of butane on the surface of alumina. It was found that excitation of the asymmetric C—H stretching modes resulted in much more desorption than excitation of the symmetric C—H stretching modes, indicating either an interesting orientation effect or a vastly different rate of VR between the two C—H modes in the same molecule.

Another important laser–surface interaction involves the process of laser ablation. Intense heating or possibly bond dissociation, caused by laser irradiation, can be used to ablate material off the surface of a solid.[36] Laser ablation is a versatile technique for micromachining of surfaces and is also used to vaporize nonvolatile materials such as high-T_c superconductors for thin-film deposition. Laser ablation is an example of a spatially inhomogeneous reaction. In such reactions it is advantageous to improve the apparatus of Fig. 3(a) by using a spatially sensitive detector that can give an ultrafast image of the process under study.[37] The apparatus in Fig. 3(a) gives data of the form $I(t_d)$, where I is an intensity variable. An ultrafast imaging apparatus, such as that described by Kim *et al.*,[37] gives data of the form $I(x, y, t_d)$.

Figure 5 is an example of a time sequence of ultrafast images obtained by using visible light as a probe. The surface of a piece of Plexiglas is irradiated by 100-psec pulses at intensities of $\sim$50 GW/cm^2. The laser pulse has a small diameter, roughly 50 μm, so that ablation from the sample occurs only in the small volume near the center of the image. The series of time-dependent images shows the formation of a hypersonic (roughly mach 20) shock wave propagating outward radially from the ablation region and, at longer

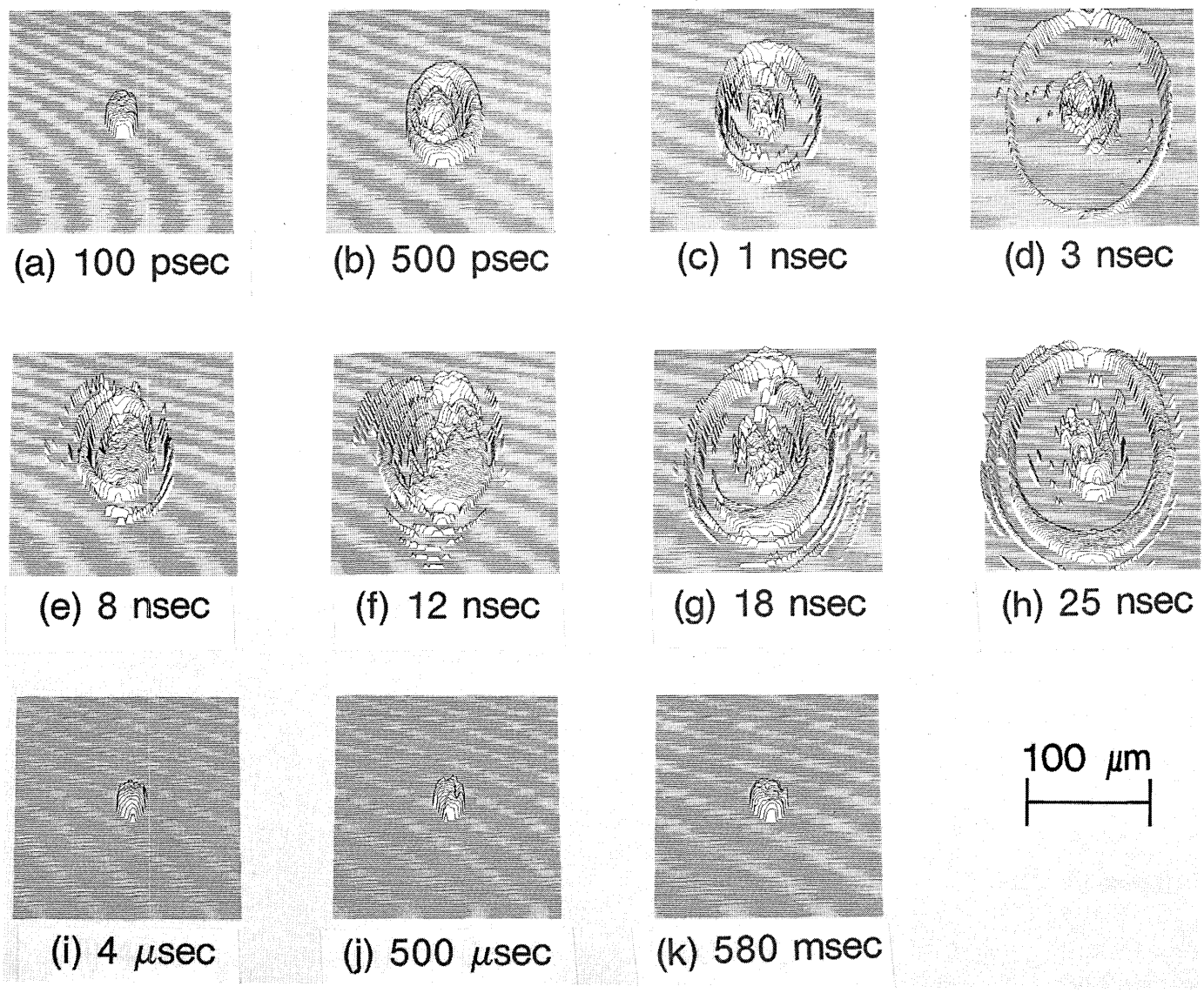

Fig. 5. Ultrafast time-resolved images of surface ablation processes obtained by Kim *et al.*[37]

delay times, the propagation of a large-amplitude acoustic wave outward from the center of the image. The mechanism used to observe these laser-produced waves was attenuation of a visible probe pulse. This probing technique does not provide chemical sensitivity, as does IR or Raman spectroscopy.

One of the most promising applications of the FEL is its use as a laser source for ablation, particularly of biological tissues in surgical applications. One reason for this promise is that FEL's provide tunable radiation that can be used to vary the penetration depth of the incident radiation on the tissues. A powerful technique for studying such processes would be the use of the FEL as a source for ultrafast imaging, using as a probe the tunable IR pulses. For example, with reference to Fig. 5, the probe could be systematically tuned into resonance with various chemical compounds such as H_2O, CO, and NH_3 expected to result from an ablation process. In this case it should be possible to produce time- and spatial-dependent maps of the concentration of each compound.

C. Photobiology and Biophysics

1. Photosynthesis and Vision

Photobiology[38] is the study of photochemical reactions in biological systems, the most noteworthy of which are photosynthesis and vision. Most photosynthesis is chlorophyll based, but there also exists in nature a unique bacterial photosynthetic system. Bacteriorhodopsin (BR) is the sole protein contained in the purple membrane from the bacterium *Halobacterium halobium*, and it has been the focus of intense investigation both because of its efficiency in synthesizing adenosine diphosphate (ATP) and because the chemistry of BR is intimately related to the chemistry of vision. Bacterial photosynthesis and vision are both based on the photochemical isomerization of retinal. A diagram of the BR chromophore is shown in Fig. 6(a). The chromophore consists of the retinal pigment, which is purple in color and absorbs throughout the visible spectrum. The pigment is bound to a membrane-based protein, which is not shown in detail. If BR is kept in the dark, the chromophore adopts

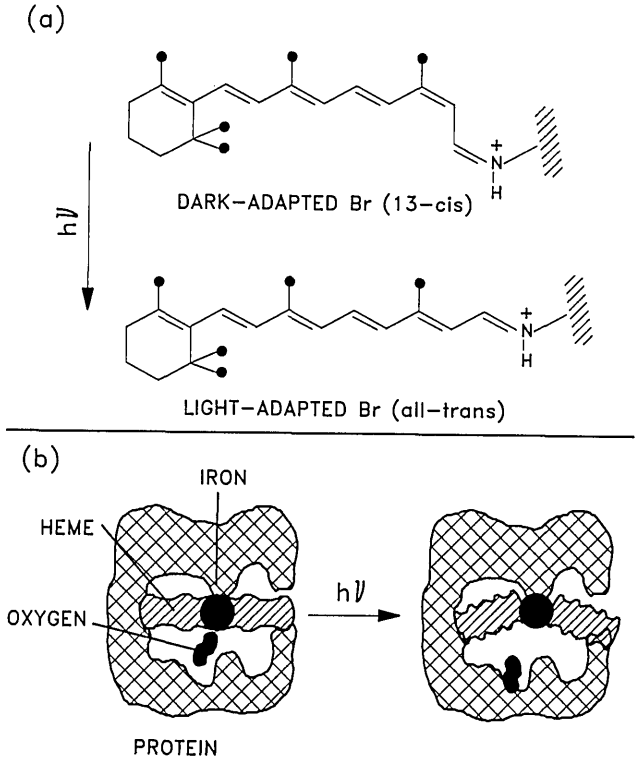

Fig. 6. Schematic diagrams of two important processes in photobiology. (a) Light-induced isomerization of BR is the primary process in bacterial photosynthesis. (b) Light-induced photodissociation and the subsequent rebinding of small ligands such as O_2 bound to heme proteins is an important method used to study protein dynamics.

the *cis* configuration shown in Fig. 6(a). When BR is allowed to adapt to light, a roughly 50:50 mixture of the *cis* and *trans* isomers is found.[38,39]

When BR absorbs a photon, the energy released by the *cis*-to-*trans* isomerization is transferred to the protein and through a poorly understood chain of events causes a proton, H^+, to be transported across the purple membrane. This microscopic proton pump creates a potential that is used to synthesize the high-energy compound ATP from adenosine diphosphate. The ATP is the fuel for almost all biochemical reactions. The primary processes in vision occur along similar lines.

The BR system has been extensively studied by ultrafast spectroscopy. The initial *cis*-to-*trans* isomerization occurs within just a few picoseconds, but the resulting chemical reactions continue for milliseconds. Because the absorption spectrum of BR is broad and nearly featureless, only vibrational spectroscopy has the potential to resolve the structural details occurring at short times. A number of workers have used resonance Raman and IR spectroscopies to compare the dark- and light-adapted BR. Resonance Raman[18] studies involve Raman scattering from the retinal chromophore using laser light that is in resonance with the $S_0 \rightarrow S_1$ transition. This provides a large increase in effective cross section and makes it possible to obtain Raman spectra in a system where the chromophore is not present in high concentration. Resonance Raman studies have been performed on the 25-psec time scale. An important drawback of this technique is that it furnished little information about the protein and membrane, as they are not highly colored and do not produce a resonance Raman spectrum. Conversely, conventional Raman studies of the protein and membrane system are hindered by the chromophore, which absorbs laser light throughout the visible spectrum. Despite heroic attempts, time-resolved IR studies of BR have been limited to the millisecond time scale.[39]

Workers in this area have produced a wide variety of isotopically substituted BR analogs by total synthesis of the retinal chromophore or by growing the membrane in cultures with isotopically labeled amino acids.[39] The biggest experimental difficulties in this area stem from the lack of suitable laser sources, again suggesting the importance of the FEL.

Resonance Raman studies of BR generally involve two synchronously pumped, cavity-dumped dye lasers.[18] One laser initiates isomerization, and the other probes the Raman spectrum of the photoproducts. High-repetition-rate lasers do not produce enough pulse energy to produce sufficient concentrations of products, while low-repetition-rate lasers do not give good signal-to-noise ratios. The FEL combines large pulse energies with high repetition rates. The FEL can also produce these large pulses in the near-IR region, where high-average-power ultrafast lasers do not yet exist. Raman scattering using near-IR sources avoids the strong absorption of the chromophore, permitting observation of the surrounding protein. This technique would seem to be an important method to study the details of the interaction between the retinal and the protein. For example, one might initiate the isomerization and use anti-Stokes probing to try to determine to which protein vibrational states the energy is transferred most efficiently.

The most effective current method for getting at the details of protein dynamics involves IR difference spectroscopy.[39] A protein is a complicated molecule with tens of thousands of normal modes, and the IR spectrum of the protein is so crowded that few individual features can be distinguished. However, when the IR spectrum of a dark-adapted protein is subtracted from the IR spectrum of a light-adapted protein, only those vibrational modes that undergo a significant perturbation on photoisomerization are visible in the difference spectrum. Dollinger *et al.* have used this technique to detect vibrational modes of an amino acid, tyrosine, which changes in position or intensity on photolysis.[39] The most diagnostically useful bands are at $\approx$1480 and $\approx$1277 cm^{-1}, a frequency regime where ultrafast visible–IR measurements cannot be made with existing laser sources.

Similar arguments can be made for chlorophyll-based photosynthetic systems, in which optical excitation of the so-called antenna pigments is funneled into a special pair of chlorophyll molecules that undergo ultrafast electron transfer processes.[38] It is a fair statement that the photosynthesis community eagerly awaits access to a laser source that is powerful enough and flexible enough to solve the mystery of the initial events in photosynthesis and vision.

2. *Heme Protein Kinetics*

Another interesting area in photobiology is the reaction of heme proteins with ligands.[40] Heme proteins are a versatile group of proteins that contain heme, an organometallic com-

pound with a highly intense absorption spectrum in the visible. Heme proteins have many functions in biology, including the storage and transport of oxygen, hydrocarbon oxydation, and electron transfer.[40]

Figure 6(b) is a schematic diagram of a typical heme protein. The protein consists of an organoiron complex, the heme, bound to a globular protein, the globin. A common heme protein found in blood is hemoglobin (Hb). The Hb molecule is tetrameric, consisting of four subunits, each similar to the monomeric protein diagrammed in Fig. 6(b).

Two extremely interesting aspects of heme protein research are peptide control of the reactivity of the active site and cooperativity. Different heme proteins possess vastly different chemical functions, but structurally they are a good deal alike. Subtle differences in the protein matrix can dramatically alter the chemistry of the heme. Cooperativity refers to communication among the tetrameric subgroups of Hb. When blood Hb is in the lungs, it must eagerly bind four O_2 molecules, but when the O_2 is required for biochemical functions, Hb must just as eagerly surrender all four molecules. When a heme subgroup binds or donates O_2, it transmits mechanical impulses to the other groups that have a strong influence on their affinity for O_2.[40]

Photochemical studies of heme–ligand kinetics are illustrated in Fig. 6(b). A ligand, usually O_2 or CO, is bound to a heme protein. When irradiated with visible light the heme is excited, and the ligand is promptly photodissociated. The dissociated ligand is propelled into the heme pocket, an inner cavity in the protein where heme resides. From the pocket, the ligand might migrate through the protein matrix, and then through the aqueous medium, to encounter another protein. Alternatively the ligand might rebind directly to the iron. The direct process is called geminate rebinding. Heme–ligand kinetics can be studied by photolyzing the heme–ligand complex and monitoring the reappearance of the bound complex. Recall that Hb that is bound to O_2 has the rich red color of arterial blood, while O_2-deficient Hb has the bluish color of venous blood; differential optical absorption studies using the apparatus of Fig. 3(a) can measure the rebinding of ligands to photolyzed heme proteins.[41,42]

Figure 6(b) shows that when O_2 heme is photolyzed, the heme group relaxes from a planar configuration (liganded) to a domed configuration (deliganded). Recent studies show that this relaxation process occurs within 350 fsec.[42] When the heme domes, it pulls on the globin at several points of attachment, and this abrupt mechanical impulse is thought to be capable of influencing the behavior of the adjacent subunits in the Hb protein.[25]

Experimental studies of heme–ligand kinetics suffer from the same problems as photosynthesis studies. Optical studies provide little information about the details of structural rearrangements, while resonance Raman studies provide important information about the heme but little about the colorless protein matrix. The availability of the FEL again suggests a number of new experiments. For example, a visible photon can be used to dissociate heme–ligand complexes, and near-IR Raman probing or IR probing[43] can be used to detect the arrival of excess vibrational energy in the surrounding protein matrix. The IR difference technique would reveal which protein modes are most strongly affected by ligand binding. Such experiments would be the first to reveal the details of this molecular machine, so vital to life, which are inaccessible to experimenters armed solely with conventional laser systems.

D. Optical Coherence

The spectroscopic experiments described in the previous sections perturb and probe population changes. In attempts to understand the influence of medium dynamics on the internal degrees of freedom of a molecule in a condensed-matter system, optical coherence techniques (nonlinear experiments) that examine optical dephasing can be of great value. Optical dephasing measurements are the time-domain equivalent of frequency-domain optical line-shape measurements. Optical dephasing experiments measure the influence of the time evolution of the medium on the internal state energies of the system under consideration. This in turn can be related to the nature of the structural evolution of the medium.

Recent theoretical developments with associated experimental methods are revolutionizing the way in which optical spectroscopy is used and interpreted in the investigation of solids with time-evolving structures.[43–45] In glasses, amorphous solids, complex crystals, proteins, and other condensed-matter systems, in addition to phonon-induced fluctuations of local mechanical properties, there can be much slower time-scale structural evolution. The local structures associated with a glassy or amorphous system, such as a molecular glass and an amorphous semiconductor, are not static even at very low temperatures (1.5 K). In glasses, small potential barriers separate different local mechanical configurations. Tunneling and thermal activation result in constantly changing local structures. This is in contrast to a simple crystal in which phonon-induced fluctuations occur about a single equilibrium lattice structure.

In addition to direct phonon-induced fluctuations, the changes in the local configurations of a glass, an amorphous solid, or a crystal can modulate the electronic or vibrational state energies of a molecule or atom. If the molecules were not coupled to the environment, an absorption spectrum would reveal a line broadened only by the excited-state lifetime, T_1. Since the chromophore is coupled to the environment, the energy levels fluctuate. Fluctuations produce a broader linewidth (frequency-domain description) or alternatively a shorter dephasing time (time-domain description). An absorption spectrum of a chromophore in a glass, an amorphous solid, or a crystal will also be inhomogeneously broadened. Inhomogeneous broadening is a result of the wide variety of static local environments. To extract dynamical information from the dephasing of excited chromophores, it is necessary to obtain line-shape information with inhomogeneous broadening removed.

The state energies of chromophores in a complex solid will be influenced by processes in the medium that range from the very fast to the totally static. For this reason it is necessary to consider carefully the sensitivity of various spectroscopic observables to the distribution of time scales.

Dephasing experiments have traditionally been treated with optical absorption formalisms. The optical line shape is proportional to the Fourier transform of a two-time dipole moment correlation function, while its time-domain equivalent, the optical free-induction decay, is directly proportional to this function. These experiments are sensitive to fluctuations on all time scales. In a solid, the inhomogeneous

broadening, or static contribution, will mask the dynamical information of interest. There is an entire class of line-narrowing experiments, such as photon echoes, accumulated photon echoes, hole burning, fluorescence line narrowing, and incoherent photon echoes, that is not described by two-time correlation functions. Recently the appropriate formulation for the interpretation of line-narrowing experiments has been developed.[43,45] It has been possible to derive and evaluate the correct correlation functions that properly describe these experiments. These are four-time correlation functions.[43,44]

To discuss line-narrowing experiments in detail it is necessary first to consider the photon echo,[27,46] a special and unique case of all such experiments.[44] The experimental apparatus and pulse sequence are depicted in Fig. 7. The apparatus consists of optical systems for making the appropriate pulse sequences, controlling intensities, aiming, focusing, and delaying the timing between pulses in the sequences. The laser is tuned to the wavelength of interest in the inhomogeneous distribution of energy levels. The first high-powered pulse in the sequence takes states within the laser interaction bandwidth and creates a coherent superposition of the ground and excited states. At time $t_d = 0$, the collection of superposition states has associated with it a macroscopic polarization. This polarization rapidly decays owing to the inhomogeneous energy distribution. At time $t_d = \tau$ later, a second pulse is directed into the sample at a small angle relative to the first pulse. The second pulse affects the phase relationships among the superposition states in a manner that reverses the inhomogeneous dephasing process. At a time $t_d = 2\tau$, the initial phase relationship among the superposition states is reestablished. Thus the macroscopic polarization is regenerated. This macroscopic polarization produces a third pulse of light, which, because of wave vector matching conditions, leaves the sample in a unique direction. The third pulse of light is the photon echo signal. The echo pulse sequence removes static inhomogeneity from the optical dephasing measurement. It measures optical dephasing induced by random fluctuations on the time scale of τ.

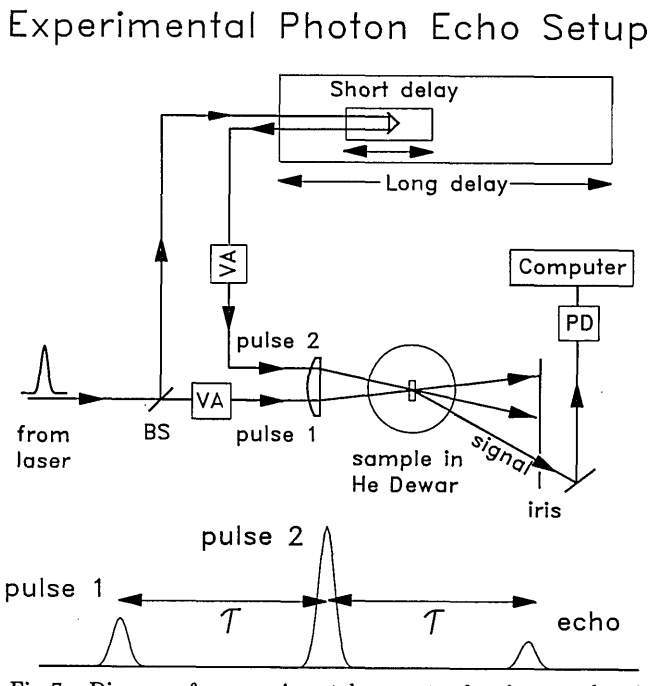

Fig. 7. Diagram of an experimental apparatus for picosecond optical coherence measurements. Pulse 2 is directed into a corner cube mounted on a motorized micrometer-driven translation stage, which permits precision delays as long as 330 psec. The stage sits atop a motor-driven carriage mounted upon a precision optical rail, which permits as much as 10 nsec of delay without optical realignment. VA's, Variable attenuators; PD, photodetector; BS, beam splitter.

There are two time scales in all the other optical line-narrowing experiments. The first is τ, as in the echo experiment. The second is a much longer waiting time, T_W. Optical experiments describable in terms of the four time-correlation functions will eliminate static inhomogeneous broadening but will be sensitive to slow dynamics on times up to T_W. For fluorescence line narrowing, T_W is of the order of the fluorescence lifetime. For accumulated photon echoes, T_W is of the order of the duration of the string of pulses used in the experiment, or of the lifetime of a bottleneck state, whichever is shorter.[44] In a hole-burning experiment, T_W is of the time scale required to write and read the hole. The photon echo experiment is unique because $T_W = 0$. Therefore the echo experiment, in a system in which dynamics occur on a wide distribution of time scales, will yield the narrowest spectroscopic line. It is sensitive to only the fastest dynamics on the time scale of τ.

The recent theoretical work provides a detailed understanding of what the various experiments actually measure and shows, contrary to popular belief, that these techniques are not equivalent. Of more importance is the fact that we now have a framework for going from the results of a combination of experiments to a detailed determination of underlying dynamics and solid-state interactions. One of the main points to come from the theoretical investigations is that a combination of experiments, particularly the photon echo and the accumulated echo, can provide information that is impossible to obtain from a single experiment. To map out the complex dynamics in solids it is necessary to do experiments on a variety of time scales. The photon echo provides the fastest time scale. The accumulated photon echo is a highly flexible method with access to a wide range of T_W. Unlike other experiments discussed above, the accumulated echo is performed with a micropulse repetition rate that is fast relative to the time for repopulation of the ground state. The ground-state recovery is limited by the kinetics of the bottleneck, often a triplet state. In the discussion below, we assume a long-lived bottleneck, for example, the 1-sec lifetime of one triplet sublevel of naphthalene.[9] The apparatus for the experiment is quite similar to that shown in Fig. 7 except that the individual pulses are replaced by strings of pulses, where the duration of each string determines T_W. In a bit of oversimplification, coherences produced at the beginning of the string contribute to the signal stimulated by pulses at the end of the string, so the coherence decay is sensitive to slow fluctuations occurring out to T_W.

By combining photon echoes with accumulated echo experiments it is possible to separate fast fluctuations from slow structural evolution.[44] Fast and slow dynamics can be cleanly separated. By changing the duration of the stream of pulses in the accumulated grating echo, the distribution of dynamical processes on different time scales can be investi-

gated. The theoretical formalism shows that the results of such an experimental combination directly yield the Laplace transform of the underlying distribution of rates of the solid's dynamical processes.[45] This approach is a fundamentally new method for examining dynamics in complex systems.

The FEL, with its ability to produce high-intensity tunable picosecond pulses, is ideally suited to perform photon echoes, accumulated echoes, and other nonlinear experiments on broad classes of interesting materials. These include the electronic states of amorphous and layered semiconductors, vibrational and electronic states of molecules in solids, vibrational and electronic states of molecules absorbed on surfaces, vibrational states of proteins, and electronic states of chromophores in proteins, to name a few.

Glasses are not equilibrium systems like crystals. Amorphous silicon is a semiconductor glass. It will not have a static structural configuration. On time scales much longer than the phonon-induced homogeneous dephasing time, slow, thermally induced structural rearrangements will contribute to changes of the energies of localized optical excitations. In discussions of amorphous semiconductors, defect states are frequently described as if they were a static set of sites in the sample. Evolution of structure, however, can cause a deep defect subsequently to become part of the conduction band, and vice versa. The question of long-time-scale structural evolution, as opposed to short-time-scale phonon-induced energy fluctuations, has not been addressed in amorphous semiconductors and is only beginning to be addressed in other systems.

The FEL at Stanford University has an optical macropulse structure that is ideally suited to performing both photon echo experiments and accumulated echo experiments. For these measurements, a string of pulses with variable pulse number is required. A pulse switch can be used to create strings with durations as long as the macropulse period, ~10 msec in the visible. In the vibrational IR, the FEL can be operated continuously, so there is no limit to the duration of the pulse string.

In addition to the accessibility of IR wavelengths, the pulse structure of the FEL makes it desirable for performing nonlinear-optical experiments. The FEL can produce pulses that are short (2 psec) and have microjoule energies. Conventional lasers can produce short high-energy pulses but only at low repetition rates. An experiment such as the accumulated echo requires a string of closely spaced pulses. This is available in the visible only at low pulse energies, which limits the usefulness of the pulse sequence. It is not available at all in the IR.

Electronic transitions of atoms and molecules have been the focus of most picosecond optical coherence experiments. Such experiments have been conducted using wavelengths in the visible spectrum because of the limitations of conventional picosecond lasers. The FEL, however, can now provide picosecond pulses of megawatt peak powers far into the IR. In addition to the experiments on localized electronic states in glasses described above, the FEL can be used to extend optical coherence experiments to vibrational states of molecules in condensed-matter systems.

In a complex system of molecules, i.e., a glass, a crystal, or a surface, dynamical intermolecular interactions play a fundamental role in determining system properties. Photon echo experiments on optical chromophores in glasses are providing detailed information on the influence of a glass's two-level system[47] dynamics on the electronic states of chromophores.[43,48] These experiments yield only indirect information on the dynamics of the two-level systems themselves. By performing photon echo experiments on the vibrational states of the molecules that form a glass, it should be possible to obtain more direct information on the glass. Comparison between the temperature-dependent dephasing of vibrational modes of the glass molecules (such as the O—H stretching mode of ethanol in an ethanol glass) and the optical dephasing of a localized electronic state in the same glass will greatly increase our understanding of solvent dynamics and the influence of solvent dynamics on electronic state energies.

Another important area of condensed-matter research is the dynamics of molecules or molecular groups on surfaces. The application of photon echo and accumulated echo experiments to molecules on surfaces has the potential to reveal the dynamics and nature of interactions between the surface and the molecules. An interesting system for study, for example, would be the silica surface OH groups in Fig. 4. Recent IR spectroscopy experiments have provided provocative insights into this system.[35] By doing combinations of picosecond photon echo and picosecond transient grating experiments on the OH stretching mode as a function of temperature, it will be possible to obtain information on the population and dephasing dynamics of this group bound to the surface. A distinct but related experiment is to examine CO bound to the iron in heme proteins,[49] using photon echo experiments. By performing the photon echo on the CO stretching mode, it should be possible to investigate the nature of the heme and protein motions that couple to the CO.

The experiments to examine vibrational dynamics in glasses, surfaces, and proteins will require tunable IR radiation at wavelengths appropriate to excite the vibrational fundamental modes of the groups of interest. These will be in the range of 3 to 15 μm. In addition, it is necessary to have picosecond pulses with sufficiently high peak power to perform optical nonlinear experiments. These requirements make the FEL well suited for this type of research.

ACKNOWLEDGMENTS

The research of D. D. Dlott was supported by the U.S. Army Research Organization through grant DAALO-86-K-0135 and by the National Science Foundation through grant NSF DMR 87-21243. It was performed while he was on sabbatical at Stanford University. He gratefully acknowledges support provided by MDF through grant N00014-85-K-0409 from the U.S. Office of Naval Research, Physics Division.

The research of M. D. Fayer was supported by the U.S. Office of Naval Research through grant N00014-86-K-0825.

Correspondence should be addressed to D. D. Dlott.

REFERENCES

1. S. L. Shapiro, ed., *Ultrashort Light Pulses*, 2nd ed. (Springer-Verlag, Berlin, 1984).
2. H. A. Schwettman and T. I. Smith, J. Opt. Soc. Am. B 973–976 (1989).

3. G. R. Fleming, *Chemical Applications of Ultrafast Spectroscopy* (Oxford U. Press, New York, 1986).
4. J. P. Heritage, J. Appl. Phys. **34,** 470 (1979).
5. A. Laubereau, L. Greiter, and W. Kaiser, Appl. Phys. Lett. **25,** 87 (1974); S. R. Shen, ed., *Non-linear Infrared Generation* (Springer-Verlag, Berlin, 1977).
6. T. Elsaesser and W. Kaiser, Chem. Phys. Lett. **128,** 231 (1986).
7. M. Berg, A. L. Harris, J. K. Brown, and C. B. Harris, Opt. Lett. **9,** 50 (1984).
8. J. B. Birks, *Photophysics of Aromatic Molecules* (Wiley-Interscience, New York, 1970).
9. S. P. McGlynn, T. Azumi, and M. Kinoshita, *Molecular Spectroscopy of the Triplet State* (Prentice-Hall, Englewood Cliffs, N.J., 1969).
10. I. B. Berlman, *Handbook of Fluorescence Spectra of Aromatic Molecules*, 2nd ed. (Academic, New York, 1971).
11. W. Demetroder, *Laser Spectroscopy, Basic Concepts and Instrumentation* (Springer-Verlag, Berlin, 1982).
12. J. R. Hill, E. L. Chronister, T.-C. Chang, H. Kim, J. C. Postlewaite, and D. D. Dlott, J. Chem. Phys. **88,** 949, 2361 (1988).
13. K. A. Peterson, M. B. Zimmt, S. Linse, R. P. Domingue, and M. D. Fayer, Macromolecules **20,** 168 (1987); R. Kopelman, S. Parus, and J. Prasad, Phys. Rev. Lett. **16,** 1742 (1986).
14. S. Califano, V. Schettino, and N. Neto, *Lattice Dynamics of Molecular Crystals* (Springer-Verlag, Berlin, 1981).
15. F. A. Cotton, *Chemical Applications of Group Theory*, 2nd ed. (Wiley-Interscience, New York, 1971); E. B. Wilson, Jr., J. C. Decius, and P. C. Cross, *Molecular Vibrations, The Theory of Infrared and Raman Vibrational Spectra* (Dover, New York, 1955).
16. E. R. Lippincott and E. J. O'Reilly, J. Chem. Phys. **23,** 238 (1955).
17. R. T. Morrison and R. N. Boyd, *Organic Chemistry*, 2nd ed. (Allyn and Bacon, Boston, Mass., 1970).
18. See, for example, R. J. H. Clarke and R. E. Hester, eds., *Advances in Infrared and Raman Spectroscopy* (Wiley, New York), particularly Vols. 7 (1980), 9 (1982), and 11 (1984).
19. D. D. Dlott, in *Laser Spectroscopy of Solids II*, W. Yen, ed., Vol. 65 of Topics in Applied Physics (Springer-Verlag, Berlin, 1989), pp. 167–200; S. P. Velsko and R. M. Hochstrasser, J. Chem. Phys. **82,** 153 (1985); J. Phys. Chem. **89,** 2240 (1985).
20. J. R. Hill and D. D. Dlott, J. Chem. Phys. **89,** 830, **89,** 841 (1988).
21. W. J. Tomlinson, R. H. Stolen, and C. V. Shank, J. Opt. Soc. Am. B **1,** 139 (1984).
22. J. Shah, IEEE J. Quantum Electron. **QE-24,** 276 (1988).
23. D. E. Cooper, R. W. Olson, R. D. Wieting, and M. D. Fayer, Chem. Phys. Lett. **67,** 41 (1979).
24. A. Laubereau and W. Kaiser, Rev. Mod. Phys. **50,** 608 (1978).
25. J. W. Petrich, J. L. Martin, D. Houde, C. Poyart, and A. Orszag, Biochemistry **26,** 7914 (1987).
26. M. D. Fayer, Annu. Rev. Phys. Chem. **33,** 63 (1982).
27. M. Berg, C. A. Walsh, L. R. Narasimhan, and M. D. Fayer, Acc. Chem. Res. **20,** 120 (1987).
28. N. H. Gottfried and W. Kaiser, Chem. Phys. Lett. **101,** 331 (1983).
29. A. Yariv, *Quantum Electronics*, 2nd ed. (Wiley, New York, 1975).
30. T. J. Kosic, R. E. Cline, Jr., and D. D. Dlott, J. Chem. Phys. **81,** 4932 (1984).
31. T. J. Chuang, G. W. Hoffman, and K. B. Eisenthal, Chem. Phys. Lett. **25,** 201 (1974); C. L. Brooks III, M. W. Balk, and S. A. Adelman, J. Chem. Phys. **79,** 784 (1983); C. L. Brooks III and S. A. Adelman, J. Chem. Phys. **80,** 5598 (1984); A. L. Harris, M. Berg, and C. B. Harris, J. Chem. Phys. **84,** 788 (1986), and references therein.
32. H. Frauenfelder and P. G. Wolynes, Science **229,** 337 (1985), and references therein.
33. N. J. Tro, D. A. Arthur, and S. M. George, J. Chem. Phys. (to be published).
34. A. C. Beri, T. F. George, J. Chem. Phys. **87,** 4147 (1987).
35. E. J. Heilweil, M. P. Cassassa, R. R. Cavanagh, and J. C. Stevenson, Chem. Phys. Lett. **117,** 185 (1985); J. Chem. Phys. **82,** 5216 (1985); **85,** 5004 (1986).
36. R. Srinivasan, Science **234,** 559 (1986).
37. H. Kim, J. C. Postlewaite, T. Zyung, and D. D. Dlott, J. Appl. Phys. **64,** 2955 (1988).
38. T. Kobayashi, ed., *Primary Processes in Photobiology* (Springer-Verlag, Berlin, 1987).
39. G. Dollinger, L. Eisenstein, S.-L. Lin, K. Nakanishi, and J. Termini, Biochemistry **25,** 6524 (1986).
40. E. Antonini and M. Brunori, *Hemoglobin and Myoglobin in Their Reactions with Ligands* (North-Holland, Amsterdam, 1971).
41. R. H. Austin, K. W. Beeson, L. Eisenstein, H. Frauenfelder, and I. C. Gunsalus, Biochemistry **14,** 5355 (1976).
42. J. L. Martin, A. Migus, C. Poyart, Y. Lecarpentier, R. Astier, and A. Antonetti, Proc. Natl. Acad. Sci. USA **80,** 173 (1983).
43. M. Berg, C. A. Walsh, L. R. Narasimhan, K. A. Littau, and M. D. Fayer, J. Chem. Phys. **88,** 1564 (1988).
44. Y. S. Bai and M. D. Fayer, Phys. Rev. B **37,** 10440 (1988); Chem. Phys. (to be published).
45. Y. S. Bai and M. D. Fayer, Phys. Rev. B (to be published).
46. I. D. Abella, N. A. Kurnit, and S. R. Hartmann, Phys. Rev. **141,** 391 (1966).
47. P. W. Anderson, B. I. Halperin, and C. M. Varma, Philos. Mag. **25,** 1 (1971); W. A. Phillips, J. Low Temp. Phys. **7,** 351 (1972).
48. C. A. Walsh, M. Berg, L. R. Narasimhan, and M. D. Fayer, J. Chem. Phys. **86,** 77 (1987).
49. J. O. Alben, D. Beece, S. F. Bowne, W. Doster, L. Eisenstein, H. Frauenfelder, D. Good, J. D. McDonald, M. C. Marden, P. P. Moh, L. Reinisch, A. H. Reynolds, E. Shyamsunder, and K. T. Yue, Proc. Natl. Acad. Sci. USA **79,** 3744 (1982); A. Ansari, J. Berendzen, D. Braunstein, B. R. Cowen, H. Frauenfelder, M. K. Hong, I. E. T. Iben, J. B. Johnson, P. Ormos, T. B. Sauke, R. Scholl, A. Schulte, P. J. Steinbach, J. Vittitow, and R. D. Young, Biophys. Chem. **26,** 337 (1987).